Circulation

Evidence for Multiple Mechanisms in Human Ventricular Fibrillation

Martyn P. Nash, Ayman Mourad, Richard H. Clayton, Peter M. Sutton, Chris P.
Bradley, Martin Hayward, David J. Paterson and Peter Taggart

The online version of this article, along with updated information and services, is
located on the World Wide Web at:

http://circ.ahajournals.org/cgi/content/full/114/6/536

Evidence for Multiple Mechanisms in Human Ventricular Fibrillation

Martyn P. Nash, PhD; Ayman Mourad, PhD; Richard H. Clayton, PhD;
Peter M. Sutton, PhD; Chris P. Bradley, PhD; Martin Hayward, MS, FRCS;
David J. Paterson, DSc; Peter Taggart, MD, DSc, FRCP

Background—The mechanisms that sustain ventricular fibrillation (VF) in the human heart remain unclear. Experimental models have demonstrated either a periodic source (mother rotor) or multiple wavelets as the mechanism underlying VF. The aim of this study was to map electrical activity from the entire ventricular epicardium of human hearts to establish the relative roles of these mechanisms in sustaining early human VF.

Methods and Results—In 10 patients undergoing cardiac surgery, VF was induced by burst pacing, and 20 to 40 seconds of epicardial activity was sampled (1 kHz) with a sock containing 256 unipolar contact electrodes connected to a UnEmap system. Signals were interpolated from the electrode sites to a fine regular grid (100×100 points), and dominant frequencies (DFs) were calculated with a fast Fourier transform with a moving 4096-ms window (10-ms increments). Epicardial phase was calculated at each grid point with the Hilbert transform, and phase singularities and activation wavefronts were identified at 10-ms intervals. Early human VF was sustained by large coherent wavefronts punctuated by periods of disorganized wavelet behavior. The initial fitted DF intercept was 5.11 ± 0.25 (mean$\pm$SE) Hz ($P<0.0001$), and DF increased at a rate of 0.018 ± 0.005 Hz/s ($P<0.01$) during VF, whereas combinations of homogeneous, heterogeneous, static, and mobile DF domains were observed for each of the patients. Epicardial reentry was present in all fibrillating hearts, typically with low numbers of phase singularities. In some cases, persistent phase singularities interacted with multiple complex wavelets; in other cases, VF was driven at times by a single reentrant wave that swept the entire epicardium for several cycles.

Conclusions—Our data support both the mother rotor and multiple wavelet mechanisms of VF, which do not appear to be mutually exclusive in the human heart. (***Circulation***. 2006;114:536-542.)

Key Words: arrhythmia ■ electrophysiology ■ fibrillation ■ mapping ■ reentry

S everal mechanisms have been shown to underlie the complex activation patterns of ventricular fibrillation (VF). The multiple wavelet mechanism, originally proposed by Moe[1] to explain atrial fibrillation, implies that VF is sustained by multiple circulating unstable wavelets perpetuated by a sequence of wavebreak and self-regenerating reentry. Recent experimental studies indicate that this mechanism can sustain VF, particularly in tissue in which the action potential duration restitution curve has a steep slope.[2] A second mechanism, the "mother rotor" hypothesis, proposes that VF is maintained by a single rapid periodic source of excitation that is unable to sustain uniform 1:1 conduction through the myocardium. Instead, the mother rotor produces fibrillatory conduction with intermittent conduction block, generating multiple irregular activation patterns.[3] A hallmark of this mechanism is a stable "domain" structure in which each domain is characterized by activity at a particular dominant frequency (DF).[4] Although both mechanisms

have been demonstrated in various experimental models, their relative roles in human VF have not been established.

Mapping of VF in the intact human heart is difficult for both technical and ethical reasons, and there are few reports in the literature. A recent study in cardiac patients on cardiopulmonary bypass mapped activation wavefronts during VF over a roughly 4.5×4.5-cm region on the anterior left ventricular epicardium.[5] Only occasional reentry was observed, with overall appearances suggestive of large wavefronts with significant organization. The authors concluded that their observations were consistent with a fairly stable mother rotor outside the mapped region or with a few constantly changing reentrant pathways and that global map-

Circulation is available at http://www.circulationaha.org   **DOI: 10.1161/CIRCULATIONAHA.105.602870**

Patient Characteristics

Patient	Age, y/Gender	CAD/AVD	LAD	LCx	RCA	EF, %	Previous MI	Diabetes	β-Blocker	Calcium Blocker	ACEI	Bypass	LVDd, cm	LVDs, cm	LVPWd, cm	IVSd, cm	Aortic Gradient, mm Hg
h012	75/M	CAD	S	N	Mod	65	No	No	Yes	No	No	On	…	…	…	…	…
h027	70/M	CAD	S	N	S	72	Yes	No	Yes	No	No	On	…	…	…	…	…
h030	59/M	CAD	S (LMS)	N	S	70	Yes	No	Yes	Yes	No	Off	…	…	…	…	…
h031	62/M	CAD	Mod	S	S	66	No	Yes	Yes	No	No	Off	…	…	…	…	…
h035	67/M	CAD	S	Mod	S	60	No	Yes	Yes	No	Yes	Off	…	…	…	…	…
h041	76/M	CAD	Mild	Mod	S	62	No	No	Yes	No	Yes	Off	…	…	…	…	…
h028	77/M	AVD	N	N	N	74	No	Yes	No	No	No	Off	3.7	2.3	1.3	1.6	88
h032	73/F	AVD	N	N	N	66	No	No	No	No	Yes	Off	3.9	3.4	1.2	1.7	57
h033	87/F	AVD	N	N	N	59	No	No	No	No	No	Off	4.4	3.0	1.2	3.3	96
h043	53/F	AVD	N	N	N	67	No	No	No	Yes	No	On	3.5	5.6	1.5	1.5	80

CAD indicates coronary artery disease; AVD, aortic valve disease; LAD, left anterior descending artery; LCx, left circumflex artery; RCA, right coronary artery; EF, ejection fraction; MI, myocardial infarction; LMS, left main stem; N, no hemodynamically significant stenosis (ie, <50% narrowing); Mild, 50% to 70% stenosis; Mod, moderate (70% to 90%) stenosis; S, severe (>90%) stenosis; ACEI, angiotensin-converting enzyme inhibitor; On, during cardiopulmonary bypass; Off, before cardiopulmonary bypass; LVDd, left ventricular diastolic dimension; LVDs, left ventricular systolic dimension; LVPWd, left ventricular posterior wall diastolic dimension; and IVSd, intraventricular septum diastolic dimension.

ping would be necessary to resolve this issue. In this article, we present observations for a similar patient group in which we have performed global mapping over both the left and right ventricles during a 20- to 40-second episode of VF either immediately before or during cardiopulmonary bypass.

Methods

Patients
Ten patients 53 to 87 years of age (mean±SD, 70±10 years; 7 men) were studied during routine cardiac surgical procedures. The study was approved by the local hospital ethics committee, and written informed consent was obtained from all patients before the study. Six patients (all men) were undergoing graft procedures for coronary artery disease. Four patients were undergoing aortic valve replacement and had no hemodynamically significant coronary artery disease (>50% stenosis in any one major vessel). Individual patient details are given in the Table.

Mapping Procedure
The studies were performed after cannulation for cardiopulmonary bypass but before the beginning of bypass in 7 patients and after the beginning of bypass in 3 patients. Similar to our previous studies,[6,7] an epicardial sock with 256 electrodes (interelectrode spacing, ≈10 mm) was fitted over the left and right ventricles (Figure 1). Unipolar epicardial electrograms were sampled at 1 kHz with the UnEmap system (Uniservices Ltd, New Zealand) with the reference channel connected to the chest retractors. VF was induced with 50-Hz burst pacing, and continuous recordings were made during the first 20 to 40 seconds of VF. A typical electrogram is illustrated in Figure 1b.

Before the experiments, the electrode sock was placed over a phantom heart model, and the 3D locations of the epicardial electrodes were digitized (Figure 1c). For analysis purposes, the electrode coordinates were projected onto a cone-shaped surface surrounding the ventricles and then down onto a circular 2D polar plot. Delaunay triangulation was used to connect the neighboring electrodes of the polar plot (Figure 1d). With this triangular mesh, the electrode potentials were linearly interpolated from the electrodes onto a fine regular grid (100×100 grid points; see Figure 1e).

Signal Preprocessing
A small number of the raw electrograms near the stimulus electrodes had a characteristic exponential settling period of ≈10 seconds immediately after the burst pacing stimulus. To remove this effect and other slow variations (such as respiratory artifact) present in many of the signals, we applied the following preprocessing stage across all the signals. For each electrode, we fitted a model with a
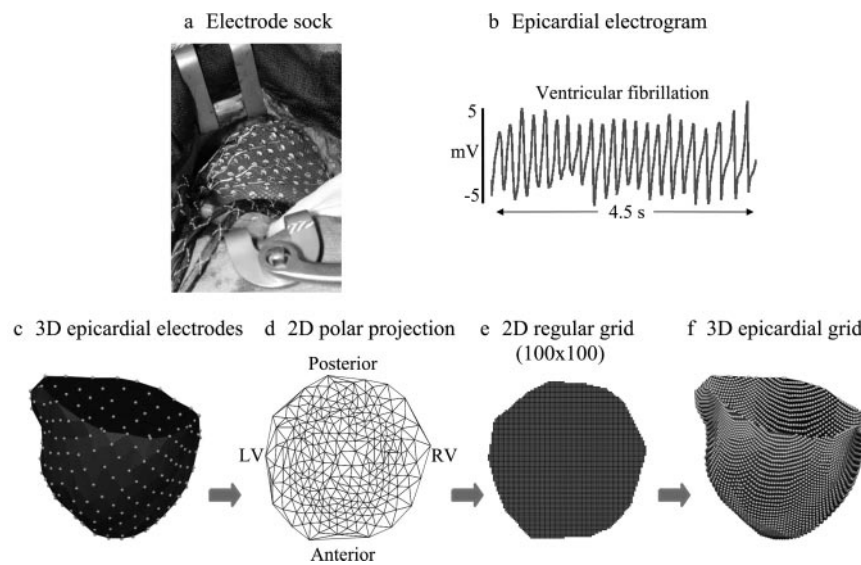
Figure 1. Epicardial mapping during VF. a, During surgery, a 256-electrode epicardial sock was connected to the UnEmap system. b, A typical epicardial unipolar electrode signal during VF. c, The 3D anatomic representation of the epicardial sock and electrode positions. d, The 2D polar projection of the ventricular epicardium with apex at the center and base at the perimeter of the map. Delaunay triangulation of the electrodes spanned the entire ventricular epicardium. e, A regular grid (100×100 points) was overlaid for each patient. For this case, 6773 grid points were contained inside the 2D epicardial map. f, Projected locations of the grid points on the 3D epicardial representation.

constant offset (signal mean), an exponential term, and a sinusoidal term (with a period of 4 seconds) to account for the respiration artifact. We then subtracted this fitted signal from the raw signal. One of the consequences of this step was that the mean of each preprocessed signal was very close to zero.

DF Analysis

DFs were computed for each electrode signal using the fast Fourier transform with a rectangular window size of 4096 ms. DF was calculated as the frequency of the dominant peak in the power spectrum. This provided a frequency resolution of ≈0.24 Hz. We used the spectrogram to represent each signal in the time-frequency domain. The temporal evolution of mean DF was determined with a window shift increment of 10 ms.

Selection of Electrograms

A proportion of the signals had poor signal-to-noise ratios, which typically were due to poor electrical contact with the ventricular tissue. We used the fast Fourier transform data to reject these signals because the main source of noise was a combination of baseline movement and electrical interference. Only signals with a DF within the range of 1.5 to 45 Hz were selected for further analysis, beginning with the signal interpolation procedure. As a result, the mean±SD number of viable electrodes was 171±41 (n=10; range, 115 to 246 electrodes; see Data Supplement Figure I).

Activation Times, Phase, Phase Singularities, and Wavefronts

Activation times were computed from the electrograms using the minimum dV/dt,[8] which varied in magnitude within and between hearts. The median value across all activations for each heart was between 0.21 and 0.46 mV/s, whereas 80% of all activations across all 10 hearts had minimum dV/dt between −1.0 and −0.05 mV/s. We assumed a minimum refractory period of 100 ms, so after an activation time, the subsequent activation for the same electrogram was assumed to occur between 100 and 300 ms later. Activation wavefronts correspond to spatial isochrones of activation time.

Phase analysis has been widely used to study electrical activity during VF because it provides a way of identifying reentrant sources that is robust in the presence of noise and changing signal morphology.[9,10] Phase transformation is achieved by plotting 2 state variables against each other. One state variable is typically the voltage; the other may be a time-delayed voltage, the rate of change of voltage, or the Hilbert transform of voltage,[11] which we used for our analysis.

One important requirement for phase analysis using the Hilbert transform is that the mean of the signal must be zero,[11] which was achieved with our signal preprocessing step. We subsequently applied a conventional linear signal detrending algorithm[12] to set the voltages at the activation times (given by minimum dV/dt) to zero. However, we noted that application of the conventional linear detrending algorithm resulted in a nonzero mean voltage, which in turn casts doubt on subsequent phase analysis. To avoid this, we modified the linear detrending algorithm[12] to include a quadratic term to ensure that the mean voltage over the interval between successive activation times was zero.

We constructed the phase plane using the Hilbert transform of the detrended signals, as illustrated in Figure 2. For a single electrode, the voltage and its Hilbert transform are shown in Figure 2a and 2b, respectively (see Data Supplement Figure II for further examples of electrograms and phase loops). The Hilbert transform was calculated for all electrodes, and the resultant data were linearly interpolated across the fine regular grid. Voltage and the Hilbert transform were plotted together in the phase plane (Figure 2c). The preprocessing step guaranteed that the central point in the phase plane was always very close to (0,0). Phase was then calculated independently for each grid point using $\varphi(t)=atan2[V(t),HV(t)]$, where $V(t)$ and $HV(t)$ represent the interpolated voltage and Hilbert transform, respectively. The spatial distributions of phase were analyzed with a topological charge technique[13] to locate the phase singularities (PSs) associated with the ends of wavefronts such as at the tip of a reentrant wave.
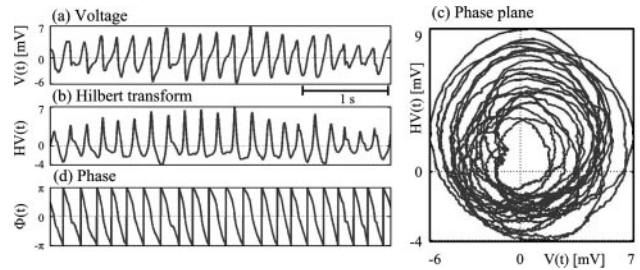
Figure 2. VF signal analysis. a, VF electrogram, V(t), with (b) its Hilbert transform, HV(t). c, Phase plane plot [V(t),HV(t)]. d, Phase, Φ(t), computed from the phase plane. Graphs in a, b, and d are plotted versus time (t). Further examples are provided in Figure II of the Data Supplement. All are plotted vs time t.

Note that after the signal detrending stage, the activation wavefronts correspond to isolines of zero voltage and hence isolines of zero phase angle under the Hilbert transform. In our hands, wavefronts determined using spatial isochrones of activation time were incompletely determined because of numerical artifact, and such problems have been previously reported.[14] Instead, we constructed activation wavefronts by tracking isolines of zero phase using an active-edge technique.[12]

Statistical Analysis

To calculate the rate at which the DF increased over time, the following procedure was used. A linear mixed model was fitted to the data. The model variable was DF, and the fixed effects for the model included an overall intercept and time. The random effects for the model were a random intercept and slope for each patient (which formed a subject group for the analysis). Fixed effects of pathology (coronary artery disease or aortic valve disease) and pathology*time were considered but were removed from the final model because they were not significant. The analysis was performed with the SAS statistical package (SAS 9.13 for Windows).

The authors had full access to the data and take full responsibility for their integrity. All authors have read and agree to the manuscript as written.

Results

Activation Waves

Wavefronts generally involved large areas of the epicardial surface in each of the recordings. Figure 3 shows a typical example of this coherent activity propagating across the ventricular epicardium from left to right. This wavefront involved
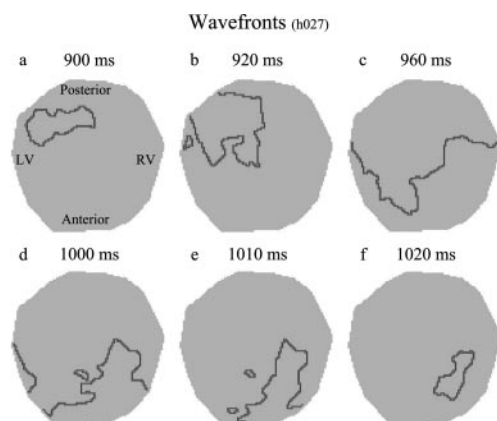
Figure 3. An example of the large coherent wavefronts observed across the ventricular epicardium during VF. Animated epicardial wavefronts during the entire VF recordings for each of the patients are shown in Data Supplement Movies I through X.
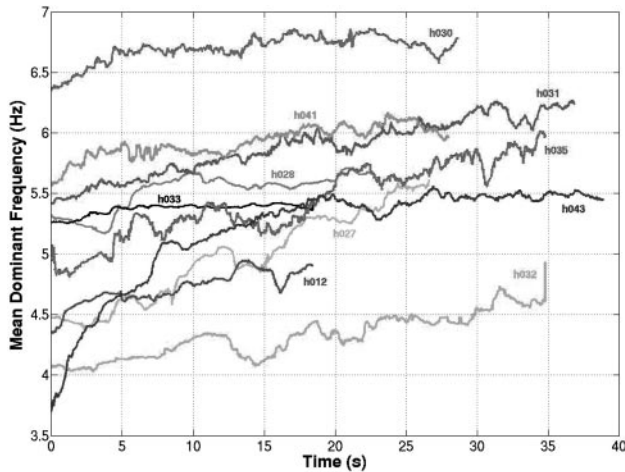
Figure 4. Temporal evolution of the global mean DF during early VF for each of the 10 patients.

almost the entire epicardial surface. Data Supplement Movies I through X show the wavefronts for each of the patients.

Overall DF

The mean DF for each recording increased over time during early VF, as illustrated in Figure 4. At the onset of VF, the fitted global mean±SE DF intercept was 5.11 ± 0.25 Hz ($P<0.0001$). During early VF, the mean DF significantly increased at a rate of 0.018 ± 0.005 Hz/s ($P<0.01$). There was no statistically significant effect of pathology on either the initial DF or the rate of change of DF.

DF Maps

Within the context of gradually increasing DF, we observed a rich variety in the spatial distribution of DF. There were 3 broad types of behavior: homogeneous-static, in which DF was spatially homogeneous and the pattern showed little change during the entire VF recording; heterogeneous-mobile, in which DF was spatially heterogeneous and the patterns of DF varied over time; and heterogeneous-static, in which DF was spatially heterogeneous but this pattern showed little change over time. Figure 5 shows examples of each type of behavior taken from 3 different patients.

In 6 patients, we observed a heterogeneous-static DF domain structure during the entire VF recording, whereas 2 patients maintained a homogeneous-static behavior during the entire VF recording. DF mobility was observed for brief periods for the remaining 2 patients. Data Supplement Movies I through X show the evolution of DF for each of the patients.

Epicardial Reentry

We observed epicardial reentry in all of the recordings, with a varying number of PSs. A very clear example of reentry is shown in Figure 6, with simultaneous snapshots of voltage (top row), phase (middle row), and PS and wavefront trajectories (lower row). Bands of equal phase can be seen to converge at a PS. Electrode traces from 4 electrodes surrounding this point are also shown in Figure 6; the arrows indicate the sequence of reentrant activation.

VF Mechanisms

The most striking finding of this study was that our observations were consistent with the idea that a single episode of human VF
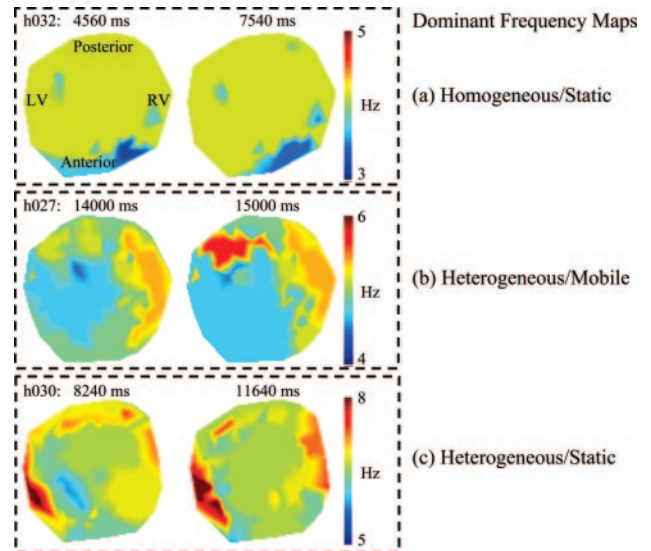

Figure 5. Examples of DF patterns from 3 patients. a, Homogeneous/static DF structure that persisted for large periods. b, Heterogeneous domains with DF mobility. c, Persistent heterogeneous/static DF domains. Animated epicardial DF patterns during the entire VF recordings for each of the patients are shown in Data Supplement Movies I through X.

could be sustained by multiple mechanisms. Figure 7 illustrates this phenomenon for 1 recording. The first column shows a snapshot in which VF was sustained by a single epicardial PS. This PS supported 5 cycles of counterclockwise reentry, and during this activity the DF map was heterogeneous-static. This period of coherent activity then degenerated. Initially, the degenerate epicardial activity was characterized by epicardial breakthroughs, as shown in the second column of Figure 7, and later it was characterized by complex patterns of wavebreak and reentry, as shown in the third column of Figure 7. This period of complex activity was associated with a heterogeneous-mobile pattern of DF. A clockwise reentrant wave then became established on the RV epicardium (fourth column of Figure 7), heralding a return to more coherent activity, which lasted for ≈20 cycles of reentry.

Multiple periods of organized epicardial reentry, epicardial breakthrough, and/or complex wavebreak activity were observed at various stages during early VF for each patient, but there was no apparent repeatability in the combinations of these behaviors within or between the fibrillating hearts.

Even during complex reentrant activity, some PSs appeared more persistent than others, as illustrated in Figure 8 for 3 different hearts. Figure 8a shows a PS that persisted on the LV epicardium of 1 heart for ≈5 seconds spanning 30 cycles. Figure 8b shows a PS that persisted on the anterior epicardium of another patient for ≈5 seconds spanning 20 cycles. This fewer number of cycles over the same time period is consistent with the lower mean DF, as illustrated in Figure 4 (compare traces for h028 against h032). Figure 8c illustrates a rapidly mobile PS as it moved from the left to right ventricular epicardium over 9 cycles in 2 seconds. In each case, the persistent PS interacted with several other short-lived PSs and wavefronts. As demonstrated in Data Supplement Movies I through X, persistent epicardial rotors (PSs) were present in all hearts regardless of pathology, and approximately equal numbers of these persistent
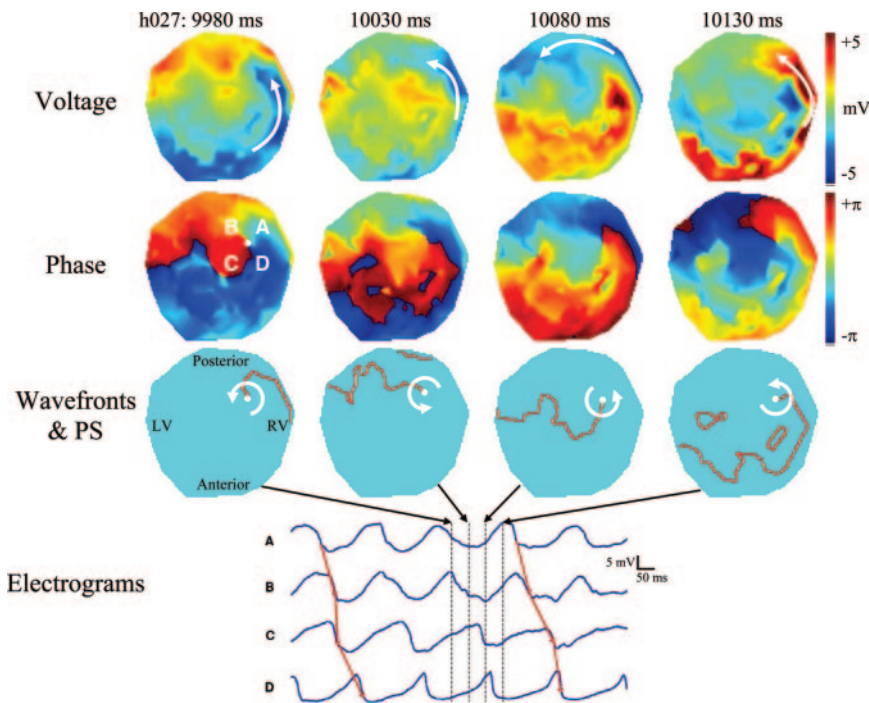
Figure 6. Reentrant activity during early VF. Epicardial distributions of electrode voltage, phase, and wavefronts and PS are illustrated (black and white circles indicate clockwise and counterclockwise chirality, respectively). Snapshots were extracted at 50-ms intervals during 1 complete cycle of a typical reentrant wave with a period of rotation of ≈200 ms. Electrode recordings from 4 electrodes surrounding the PS illustrate the relationship between signal morphologies.

rotors were stationary (such as that illustrated in Figure 6) and mobile (such as that in Figure 8c). Over all patients, we typically observed low numbers of epicardial PSs, as illustrated in Figure 8d, with 0 epicardial PS present for ≈4% of the time, just 1 PS present for 4% of the time, ≤5 PSs for 43% of the time, and ≤10 PSs for 84% of the time.

Discussion

This study mapped the entire ventricular epicardium during early human VF. We found that VF was sustained predominantly by reentry. During a single episode of VF, we observed that activity was at times driven by a single epicardial reentrant source, whereas at other times, multiple reentrant sources sustained the fibrillatory activity. We conclude that there is evidence for both mechanisms of VF in the human heart and that these mechanisms are not mutually exclusive.

Size of Activation Waves

In a previous study of VF in the human heart, Nanthakumar et al[5] showed repeatable large wavefronts on a portion of the anterior ventricular epicardium. Our findings are consistent with this observation (Figure 3) and extend this idea to the entire human ventricular epicardium. This finding, together with other studies that measured activity on the human ventricular endocardium,[15] indicates that human VF is characterized by activation wavefronts that tend to be large and coherent.

Dominant Frequency

The mean DF increased during VF in all patients (Figure 4). Studies of the body surface ECG during the initial stages of spontaneous human VF have reported comparable findings.[16] This is consistent with the interpretation that the burst pacing–induced fibrillation in the present study is similar to
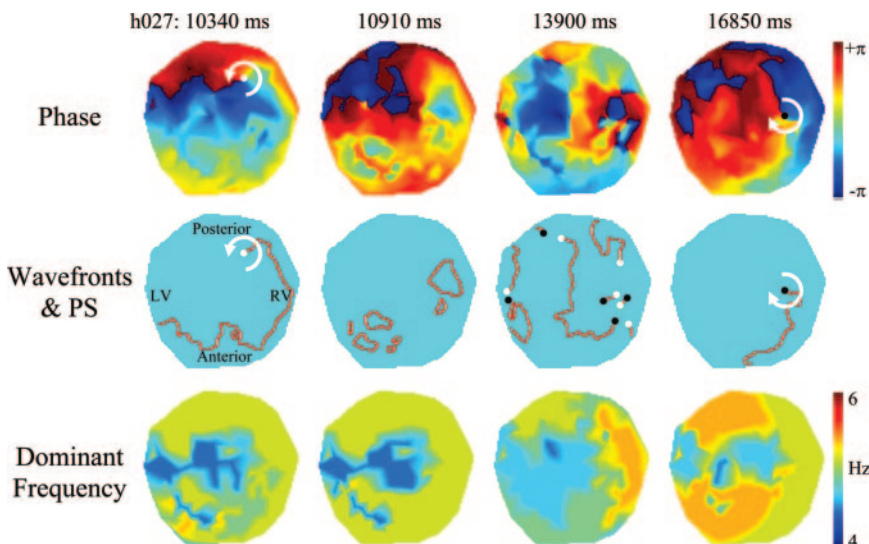
Figure 7. A variety of VF activity patterns. Rows illustrate spatial distributions of phase, the corresponding wavefronts, PS (black and white circles indicate clockwise and counterclockwise chirality, respectively), and DF. Column 1, Counterclockwise epicardial reentry. Column 2, Multiple breakthrough activity that consisted primarily of epicardial breakthrough patterns (consistent with endocardial to epicardial propagation). Column 3, Complex interactions of several reentrant sources and disorganized activity. Column 4, A clockwise reentrant wave annihilated all other sources to dominate the epicardial activity. Animated wavefront patterns during the entire VF recordings for each of the patients are shown in Data Supplement Movies I through X.
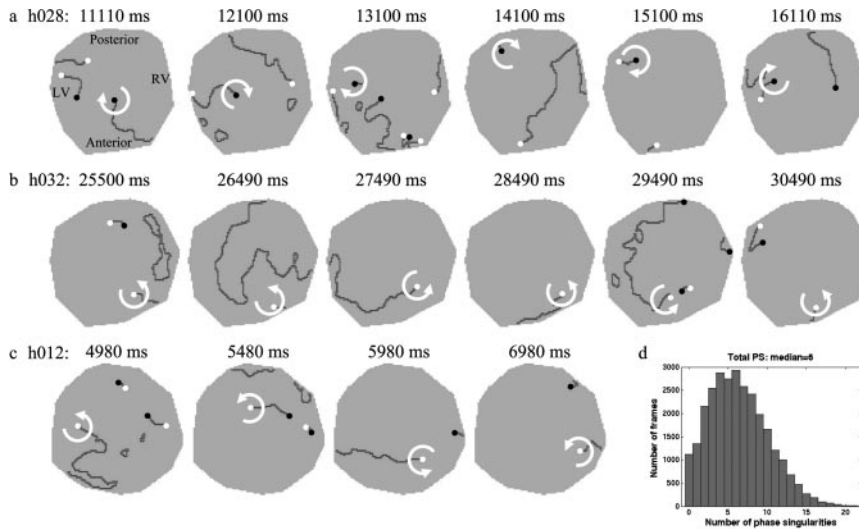
Figure 8. a–c, Examples of persistence of epicardial rotors (PS) among complex wavebreak activity during early VF in 3 patients. Black and white circles indicate clockwise and counterclockwise chirality, respectively. d, Histogram of numbers of epicardial rotors present in each frame (snapshots taken at 10-ms intervals) tallied across all patients. See text for details.

spontaneously initiated VF. It is known that as VF progresses, DF decreases, which is believed to be as a result of progressive ischemia.[17] The mechanisms underlying the increase in DF during early VF are not clear. One possibility is that it represents an adaptation of the tissue resulting from the short cycle lengths associated with VF before the development of the electrophysiological effects of ischemia.

The spatial distribution of DF was intermittently either static or mobile and either homogeneous or heterogeneous. The various behaviors are shown in Figure 5, which illustrates DF patterns for 3 different patients. Previous experimental studies[4,18] have shown a persistent and stable pattern of VF in preparations, supporting the idea that VF is sustained by a mother rotor, whereas other studies have shown shifting patterns of DF that support the idea of multiple wavelets.[19,20] Our study indicates that during early VF in the human heart, DF patterns are generally static, although 2 patients showed periods of DF mobility. We found no general trend from stability to mobility; in other words, there was no tendency for a stable DF pattern to degenerate in a mobile pattern or vice versa. Furthermore, in the 2 patients with infarction, there was no correspondence between the location of the infarction and the spatial patterns of DF.

Reentrant Sources

In each patient, we observed periods when the configuration of reentry was stable over several cycles (see Data Supplement Movies I through X). These periods of stability were punctuated by periods of more complex activity, as illustrated in Figure 7. From this, we could speculate that the engine of VF in the human heart is a relatively small number of quasi-static reentrant sources, which periodically break down into multiple wavelets. However, a more detailed analysis is required to firmly establish this notion.

The 2 periods of stability illustrated in Figure 7 show PSs of opposite chirality located in the lateral right ventricular epicardium and suggest that in this case an anatomic obstacle may be acting to pin the reentrant source. However, the data shown in Figure 8 are from different patients and indicate that a persistent PS also could be mobile.

Study Limitations

There are 5 main limitations to this analysis. First, our measurements were limited to the epicardium only, so we were not able to locate reentrant sources on the endocardial surface or within the ventricular wall. Second, our measurements were made during cardiac surgery; therefore, we were not able to assess independently the impact of anesthesia, cannulation, or other aspects of the surgical procedure. Although we did not include signals from electrodes with poor electrical contact in our analysis, some of the voltage and phase maps showed transient features that could be artifact arising from movement of the heart. Third, as in another study of human VF,[5] the patients in this study were on a variety of drug regimens. Although these drugs may influence the VF mechanism, it should be noted that these drug regimens are typical for patients at risk of spontaneous VF. Fourth, the initiation of VF in this study was by burst pacing and thus may not correspond exactly to spontaneous VF.

The other important limitation in this study was the spatial resolution of the electrodes. Experimental studies of VF mechanisms in animal hearts typically use voltage-sensitive fluorescent dyes to map electrical activity across thousands of pixels. It is not appropriate to use such dyes for mapping the human heart because of their toxicity and the fact that electromechanical uncoupling agents are typically required. We fitted an electrode sock over the entire ventricular epicardium, and the array of contact electrodes were spaced ≈10 mm apart. This large spatial resolution could have resulted in an underestimate of the complexity of activity during human VF. However, the study of Nanthakumar et al[5] used an electrode plaque with a spacing of 2 mm. Both our results and those of Nanthakumar et al document coherent wavefronts during VF. Thus, we believe that the periods of coherent epicardial activity observed in this study (eg, Figure 6) are truly representative.

Mechanisms Sustaining Human VF

The mechanisms that sustain VF remain controversial. Some experimental studies support the idea of a single periodic source, yet others support the idea of multiple interacting wavelets.[3,17,21] Our findings from the intact, in situ human heart indicate that both mechanisms exist and are not mutually exclusive during human VF. We observed periods of VF consistent with each mechanism; an example of each is shown in Figure 7. Our approach enabled us to measure activity only on the epicardial surface; as already noted, we

could not observe activity within the ventricular wall or septum. Hence, we could not exclude the possibility of a persistent mother rotor concealed within these regions.

It was not possible in this study to identify unequivocal transitions from mother rotor to multiple wavelets. Nevertheless, the observations from this study strongly suggest that these transitions do occur. Neither a single persistent mother rotor nor a purely multiple wavelet mechanism are wholly consistent with our observations. We observed mobile DF maps, which are not consistent with a stable mother rotor,[4,19] and we observed a relatively small numbers of stable epicardial PSs, which are not consistent with the large incidence of transient wavebreak observed during multiple wavelet VF.[22] Instead, our observations are consistent with a small number of mobile or stationary reentrant sources that intermittently break up into multiple sources and then coalesce again into a small number of reentrant sources. There are possible links between this observation and modeling studies that show intermittent organization of reentry.[23]

Further studies are needed to elucidate these findings in more detail and to determine the conditions that modulate this behavior. These include increasing or decreasing mobility of reentrant sources and increasing or decreasing breakup and stability of rotors. This further work would have clinically important implications in providing a step toward defining targets accessible to therapeutic intervention.

Sources of Funding

Disclosures

None.

References

1. Moe GK. On the multiple wavelet hypothesis of atrial fibrillation. *Arch Int Pharmacodyn Ther*. 1962;140:183–188.
2. Garfinkel A, Kim YH, Voroshilovsky O, Qu ZL, Kil JR, Lee MH, Karagueuzian HS, Weiss JN, Chen PS. Preventing ventricular fibrillation by flattening cardiac restitution. *Proc Natl Acad Sci U S A*. 2000;97:6061–6066.
3. Jalife J. Ventricular fibrillation: mechanisms of initiation and maintenance. *Annu Rev Physiol*. 2000;62:25–50.
4. Zaitsev AV, Berenfeld O, Mironov SF, Jalife J, Pertsov AM. Distribution of excitation frequencies on the epicardial and endocardial surfaces of fibrillating ventricular wall of the sheep heart. *Circ Res*. 2000;86:408–417.
5. Nanthakumar K, Walcott GP, Melnick S, Rogers JM, Kay MW, Smith WM, Ideker RE, Holman W. Epicardial organization of human ventricular fibrillation. *Heart Rhythm*. 2004;1:14–23.
6. Nash MP, Bradley CP, Sutton PM, Clayton RH, Kallis P, Hayward MP, Paterson DJ, Taggart P. Whole heart action potential duration restitution properties in cardiac patients: a combined clinical and modelling study. *Exp Physiol*. 2006;91:339–354.
7. Nash MP, Bradley CP, Paterson DJ. Imaging electrocardiographic dispersion of depolarization and repolarization during ischemia. *Circulation*. 2003;107:2257–2263.
8. Haws CW, Lux RL. Correlation between in vivo transmembrane action potential durations and activation-recovery intervals from electrograms: effects of interventions that alter repolarization time. *Circulation*. 1990; 81:281–288.
9. Witkowski FX, Penkoske PA. Activation patterns during ventricular fibrillation. *Ann N Y Acad Sci*. 1990;591:219–231.
10. Gray RA, Pertsov AM, Jalife J. Spatial and temporal organization during cardiac fibrillation. *Nature*. 1998;392:75–78.
11. Bray M-A, Wikswo JP. Considerations in phase plane analysis for nonstationary reentrant cardiac behaviour. *Phys Rev E*. 2002;65:051902-1–051902-8.
12. Rogers JM. Combined phase singularity and wave front analysis for optical maps of ventricular fibrillation. *IEEE Trans Biomed Eng*. 2004;51:56–65.
13. Bray M-A, Wikswo JP. Use of topological charge to determine filament location and dynamics in a numerical model of scroll wave activity. *IEEE Trans Biomed Eng*. 2002;49:1086–1093.
14. Rogers JM, Usui M, KenKnight BH, Ideker RE, Smith WM. A quantitative framework for analyzing epicardial activation patterns during ventricular fibrillation. *Ann Biomed Eng*. 1997;25:749–760.
15. Walcott GP, Kay GN, Plumb VJ, Smith WM, Rogers JM, Epstein AE, Ideker RE. Endocardial wave front organization during ventricular fibrillation in humans. *J Am Coll Cardiol*. 2002;39:109–115.
16. Clayton RH, Murray A, Campbell RWF. Changes in the surface electrocardiogram during the onset of spontaneous ventricular fibrillation in man. *Eur Heart J*. 1994;15:184–188.
17. Chen PS, Wu TJ, Ting CT, Karagueuzian HS, Garfinkel A, Lin SF, Weiss JN. A tale of two fibrillations. *Circulation*. 2003;108:2298–2203.
18. Chen J, Mandapati R, Berenfeld O, Skanes AC, Jalife J. High-frequency periodic sources underlie ventricular fibrillation in the isolated rabbit heart. *Circ Res*. 2000;86:86–93.
19. Choi B-R, Nho W, Liu T, Salama G. Lifespan of ventricular fibrillation frequencies. *Circ Res*. 2002;91:339–345.
20. Valderrabano M, Yang J, Omichi C, Kil JR, Lamp ST, Qu ZL, Lin SF, Karagueuzian HS, Garfinkel A, Chen PS, Weiss J. Frequency analysis of ventricular fibrillation in swine ventricles. *Circ Res*. 2002;90:213–222.
21. Rogers JM, Ideker RE. Fibrillating myocardium: rabbit warren or beehive? *Circ Res*. 2000;86:369–370.
22. Valderrabano M, Chen PS, Lin SF. Spatial distribution of phase singularities in ventricular fibrillation. *Circulation*. 2003;108:354–359.
23. Zaritski RM, Mironov S, Pertsov AM. Intermittent self organization of scroll wave turbulence in three-dimensional excitable media. *Phys Rev Lett*. 2004;92:168302-1–168302-4.

CLINICAL PERSPECTIVE

The design of therapies to prevent and terminate ventricular fibrillation (VF) is limited by the lack of precise understanding of VF mechanisms in humans. VF has been studied extensively in animal models from which 2 major mechanisms are favored. One postulates that multiple self-sustaining reentry wavelets circulating through the ventricles maintain VF. A more recent suggestion is that a large single "mother rotor" exists and generates waves that break up as they propagate across the ventricles, thus creating the disorganized appearance. Detailed mapping observations in humans are limited. We recorded detailed epicardial maps of VF during 20 to 40 seconds of VF induced at the time of cardiac surgery. The findings suggest that both mechanisms occur in humans and may be present simultaneously. Because different therapeutic strategies have been proposed for each mechanism, including altering various combinations of refractoriness, and the restitution properties of action potential duration or conduction velocity, the coexistence of both mechanisms is likely to have considerable impact on any potential pharmacological approach to the prevention of VF.